IMPACT BASIN FORMATION: TESTING THE NESTED MELT-CAVITY MODEL WITH NEW CATALOGS OF PEAK-RING BASINS ON THE MOON AND MERCURY. D. M. H. Baker[1] and J. W. Head[1].
[1]Dept. Geological Sci., Brown Univ., Box 1846, Providence, RI 02912, Email: David_Baker@brown.edu.

Introduction: While there have been numerous models proposed for impact basin formation [1-2], there has been no concensus on the dominant processes controlling the observed size-morphology progression of large impact structures on the terrestrial planets. Important to constraining impact basin formation models has been morphologic catalogs of impact structures in the transition between complex craters and multi-ring basins, including peak-ring basins (exhibiting a single interior ring) and protobasins (interior ring plus a central peak) [3-6].

Recent orbital and flyby data have greatly improved portrayal of basin features. Global topographic maps of the Moon at better than 128 pixel/degree resolution from the Lunar Orbiter Laser Altimeter (LOLA) provide substantial improvements over earlier datasets [7]. MESSENGER flyby image mosaics (~500 m/pixel resolution) have nearly doubled our image coverage of Mercury's surface [8]. We have used these recent orbital and flyby image and topographic data to update the present catalogs of peak-ring basins and protobasins on both the Moon and Mercury [9-12]. We also observe a new basin type, ringed peak-cluster basin, which exhibits a diminutive interior ring of central peak elements [12]. These catalogs include measurements of basin rim-crest, ring, and central peak diameters [10-11]. Measurements were obtained from circle fits to features using the CraterTools extension for ArcMap [13]. Here, we use the main observations from these new catalogs [10-11] to test the predictions of one basin formation model, which seeks to explain the formation of basin rings by modification of the crater interior from a growing impact melt cavity.

Observations:

1. Number of basins: The Moon has 17 peak-ring basins and 3 protobasins, while Mercury has a much larger population of 74 peak-ring basins and 32 protobasins. Mercury also has the largest density of peak-ring basins (9.9 x 10^{-7} per km^2) of the terrestrial planets, and a factor of two greater density than the Moon (4.5 x 10^{-7} per km^2). There are nine ringed peak-cluster basins on Mercury and only one on the Moon.

2. Ring vs. rim-crest diameter trends: Peak-ring basins on the Moon and Mercury define similar power-law trends on a log-log plot of peak-ring diameter (D_{ring}) versus rim-crest diameter (D_r) [5] (Fig. 1). The power-law fits to peak-ring basins on the Moon and Mercury are $D_{ring} = 0.14 \pm 0.10 (D_r)^{1.21 \pm 0.13}$ (R^2 = 0.96) and $D_{ring} = 0.25 \pm 0.14 (D_r)^{1.13 \pm 0.10}$ (R^2 = 0.87), respectively. Protobasins occur at smaller rim-crest diameters, generally have smaller interior rings compared to peak-ring basins, and overlap with the rim-crest diameters of peak-ring basins and ringed peak-cluster basins on Mercury (Fig. 1). Ringed peak-cluster basins overlap in rim-crest diameter with protobasins and fall along the trends for the diameters of central peaks in complex craters [5, 14-15] (Fig. 1).

3. Ring/rim-crest ratios: Ratios of ring to rim-crest diameter have been used to suggest that peak-ring basins and protobasins form a continuum of interior morphologies [6]. This view is supported by the updated catalogs for the Moon and Mercury (Fig. 2). Peak-ring basins and protobasins on the Moon and Mercury form similar continuous, nonlinear trends

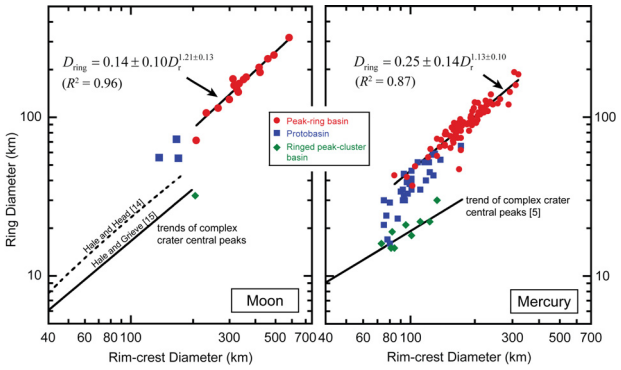

Fig. 1. Log-log plots of interior-ring diameter (D_{ring}) versus rim-crest diameter (D_r) for peak-ring basins (red circles), protobasins (blue squares), and ringed peak-cluster basins (green diamonds) on the Moon (left) and Mercury (right). Peak-ring basins on the Moon and Mercury follow similar power-law trends (see text and figure labels for equations). Protobasins occur at smaller rim-crest diameters and have smaller peak-ring diameters. Ringed peak-cluster basins appear to follow the trends of central peak diameters in complex craters [5, 14-15] and have very small ring diameters.

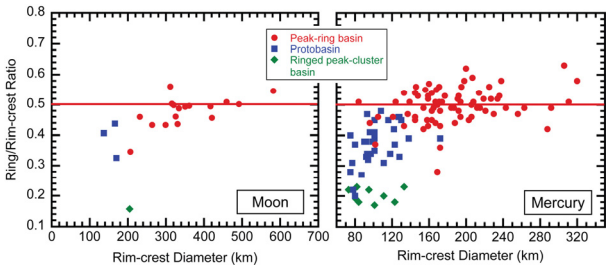

Fig. 2. Ring/rim-crest ratio versus rim-crest diameter for peak-ring basins (red circles), protobasins (blue squares), and ringed peak-cluster basins (green diamonds) on the Moon (left) and Mercury (right). A continuous, nonlinear trend is observed between protobasins and peak-ring basins on both the Moon and Mercury. Peak-ring basins have the largest ring/rim-crest ratios and flatten at about 0.5 on the Moon (left) and 0.5 to 0.6 on Mercury (right). Ringed peak-cluster basins appear to diverge from the nonlinear trend formed by protobasins and peak-ring basins and have very small ring/rim-crest ratios.

in plots of ring/rim-crest ratio versus rim-crest diameter, although basins on the Moon occur at much larger rim-crest diameters (Fig. 2). Ring/rim-crest ratios for peak-ring basins flatten to values of around 0.5 for the Moon and slightly higher values of 0.5 to 0.6 for Mercury. Protobasins generally have smaller ring/rim-crest ratios than peak-ring basins on Mercury and the Moon (Fig. 2). Ringed peak-cluster basins do not follow the continuum formed by protobasins and peak-rings, occurring at much smaller ring/rim-crest ratios (Fig. 2).

4. Rim-crest onset diameter: The term "onset diameter" has been loosely defined in the literature [5]. Here, we calculate the onset diameter for peak-ring basins as the fifth percentile of the peak-ring basin population. The Moon has the largest onset diameter (227 km) [11], followed by Mercury (116 km) [10], Mars (56 km) [4], and Venus (33 km) [6].

Testing the nested melt-cavity model: The nested melt-cavity model of basin formation is based on a suite of papers by M. Cintala and R. Grieve [16-19], which combined terres-

trial field studies with impact theory to show that impact-melt volume increases at a rate that is greater than growth of the crater volume with increasing energy of the impact event. A power-law relationship between melt volume and the final crater diameter was derived [16] and was used to show that the depth of impact melting is an important control on crater modification. Head [20] further developed this model to suggest that a melt cavity nested within the transient cavity greatly influences basin ring development. With increasing basin size, the melt cavity becomes sufficiently deep to retard development of central peaks. Peak rings form as a product of rebound and collapse of the transient cavity, which translates the melt cavity upward and inward and leaves the periphery of the melt cavity as the only topographically prominent feature. At smaller crater sizes, the depth of melting is shallower and may allow a small central peak to rise through the melt cavity, resulting in the central peak plus ring combinations that are observed in protobasins.

We find that the observations of these updated basin catalogs for the Moon and Mercury [10-11] are largely consistent with a nested melt-cavity model. First, under the nested melt-cavity model, peak ring formation will be more effective at smaller impactor sizes for planets experiencing the highest impact velocities due to the importance of velocity in determining impact melt volume. For example, impactors of a given size will produce approximately twice as much melt on Mercury than on the Moon due to Mercury's much higher mean impact velocity (42.5 km/s on Mercury and 19.4 km/s on the Moon) [18, 21]. Since small impactors are more numerous than large impactors, the surface density of peak-ring basins should increase with mean impact velocity at the planet, assuming similar impactor size distributions [22]. This may explain the factor of two larger density of peak-ring basins on Mercury compared to the Moon [20].

Second, increasing depth of melting with increasing crater size and progressive suppression of the uplifted central peak will produce a continuum of basin morphologies, from central peaks to central peak plus peak ring combinations and finally single peak rings. This size-morphology continuum between protobasins and peak-ring basins is apparent in the plots of ring/rim-crest ratios (Fig. 2).

Third, the nested melt-cavity model may be quantitatively compared to the power-law fits to peak-ring basins on the Moon and Mercury (Fig. 1). We assume a hemispherical melt cavity and use the power law relationship between melt volume and diameter of the transient cavity from [16] combined with crater modification scaling relationships [23-24] to derive a power law expression between the interior-ring diameter (D_{ring}) to the diameter of the final crater (D_{r}):

$$D_{\mathrm{ring}} = AD_{\mathrm{r}}^{p} \qquad \text{[Eq. 1]}$$

where $A = (12c/\pi)^{1/3}\ (\alpha^{d})^{1/3}$ and $p = \beta d/3$. The constants c and d are from [18] and depend on target and impactor properties. The constants α and β are from the scaling used to convert transient cavity diameters to final crater diameters. We use constants from [23] [$\alpha = (D_{\mathrm{sc}})^{0.15 \pm 0.04}$ and $\beta = 0.85 \pm 0.04$] and [24] [$\alpha = 0.980(D_{\mathrm{sc}})^{0.079}$ and $\beta = 0.921$], where D_{sc} is the simple-to-complex transition diameter on the planet [10.3 ± 4 km (Mercury) and 19 km (Moon)] [5]. Since the power-law fits in Fig. 1 follow the same form as Eq. 1, they may be directly compared for consistency with the nested melt-cavity model. Modeled values for the constant A in Eq. 1. range from 0.11 to 0.17 for the Moon and Mercury. Modeled values for p range from 1.03 to 1.18 for the Moon and Mercury. These values for A and p fall within the values (including uncertainties) obtained from power-law fits to peak-ring basins on the Moon (A = 0.04 to 0.24, p = 1.09 to 1.34) and Mercury (A = 0.11 to 0.39, p = 1.03 to 1.23) (Fig. 1). To first-order, the nested melt-cavity model offers a quantitative explanation for the ring and rim-crest diameter systematics observed from the updated basin catalogs for the Moon and Mercury [10-11].

Finally, a correlation of peak-ring basin onset diameter with planetary gravitational acceleration has favored gravity-driven basin formation models [1, 25]. Under the nested melt-cavity model, the ratio of depth of melting (d_{m}) to depth of the transient cavity (d_{tc}) is likely to be important in forming peak rings. Since gravity largely determines crater dimensions and velocity largely determines impact melt volume, both gravity and velocity should be controlling the onset of peak-ring basins. We determine $d_{\mathrm{m}}/d_{\mathrm{tc}}$ ratios of 0.7 for the Moon and 0.8 for Mercury using the relationships of [16-19] at the onset diameters for peak-ring basins. These similar high ratios are consistent with a model requiring large depths of melting for the onset of interior peak rings. Higher $d_{\mathrm{m}}/d_{\mathrm{tc}}$ ratios near 1.0 may be needed for the onset of multi-ring basins [20].

Conclusions: Observations from updated basin catalogs for the Moon and Mercury [10-11] show many consistencies with predictions of the nested melt-cavity model of basin formation [16-20]. Under this model, basin rings are formed from the nonlinear scaling of impact melt [16-19] and development of an interior melt cavity, which suppresses central peak development and forms peak rings at sufficient depth of melting. Multi-ring basins are formed [20] by even greater depths of melting, which assists mega-terracing and formation of topographic rings exterior to the transient cavity rim. While the first-order consistencies of the nested melt-cavity model are promising, much work, including advanced impact simulations, is needed for further testing of this basin formation model.

References: [1] Melosh, H.J. (1989) *Impact Cratering: A Geological Process*, Oxford Univ. Press, London. [2] Spudis, P.D. (1993) *The Geology of Multi-Ring Impact Basins*, Cambridge Univ. Press, UK, 263 pp. [3] Wood, C.A. and Head, J.W. (1976) *Proc. Lunar Sci. Conf. 7*, 3629-3651. [4] Pike, R.J., Spudis, P.D. (1987) *Earth Moon Planets*, 39, 129-194. [5] Pike, R.J. (1988) in *Mercury*, Vilas, F. et al. (eds.), Univ. Arizona Press, 165-273. [6] Alexopoulos, J.S., McKinnon, W.B. (1994) *Geol. Soc. Amer. Special Paper 293*, 29-50. [7] Smith, D.E. et al. (2010) *Geophys. Res. Lett.*, 37, L18204. [8] Becker, K.J. et al. (2009), *Eos Trans. Amer. Geophys. Un.*, 90(52), no. P21A-1189. [9] Kadish, S.J. et al. (2011) *LPS 42*, no. 1006, this volume. [10] Baker, D.M.H et al. (2011) *Planet. Space Sci.*, in review. [11] Baker, D.M.H. et al. (2011) *Icarus*, in revision. [12] Schon, S.C. et al. (2011) *Planet. Space Sci.,* in review. [13] Kneissl, T., van Gasselt, S., Neukum, G. (2010) *Planet. Space Sci.*, in press. [14] Hale, W.S., Head, J.W. (1979) *Proc. Lunar Sci. Conf. 10*, 2623-2633. [15] Hale, W.S., Grieve, R.A.F. (1982) *J. Geophys. Res.*, 87, A65-A76. [16] Grieve, R.A.F., Cintala, M.J. (1992) *Meteoritics*, 27, 526-538. [17] Cintala, M.J., Grieve, R.A.F. (1994) *Geol. Soc. Amer. Special Paper 293*, 51-59. [18] Grieve, R.A.F., Cintala, M.J. (1997) *Adv. Space Res.*, 20, 1551-1560. [19] Cintala, M.J. and Grieve, R.A.F. (1998) *Meteorit. Planet. Sci.*, 33, 889-912. [20] Head, J.W. (2010) *Geophys. Res. Lett.*, 37, L02203. [21] Le Feuvre, M., Wieczorek, M.A. (2008) *Icarus*, 197, 291-306. [22] Strom, R.G. (2005) *Science*, 309, 1847-1850. [23] Croft, S.K. (1985) *J. Geophys. Res.*, 90, C828-C842. [24] Holsapple, K.A. (1993) *Ann. Rev. Earth Planet. Sci.*, 21, 333-373. [25] Melosh, H.J. (1982) *J. Geophys. Res.*, 87, 371-380.